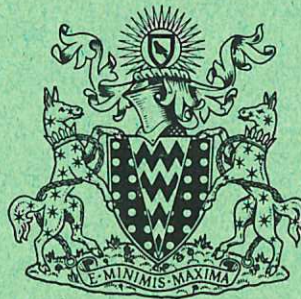
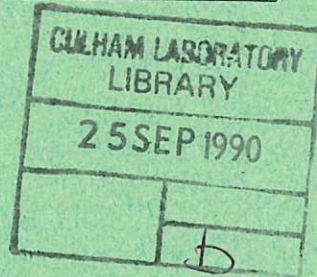


This document is intended for publication in a journal, and is made available on the understanding that extracts or references will not be published prior to publication of the original, without the consent of the authors.



UKAEA RESEARCH GROUP

Preprint

A LITHIUM COOLED TOROIDAL FUSION REACTOR

J T D MITCHELL
R HANCOX

CULHAM LABORATORY
Abingdon Berkshire

1972

Enquiries about copyright and reproduction should be addressed to the Librarian, UKAEA, Culham Laboratory, Abingdon, Berkshire, England

A LITHIUM COOLED TOROIDAL FUSION REACTOR

by

J T D Mitchell
R Hancox

Paper presented at Intersociety Energy Conversion Engineering Conference, San Diego, U.S.A. 25 September-29 September, 1972.

A B S T R A C T

A design for a deuterium-tritium fuelled fusion reactor incorporating plasma confinement in Tokamak geometry is described, in which lithium simultaneously performs the functions of neutron moderation, tritium breeding and heat removal. The limitations of the system due to MHD losses in the circulating lithium are considered in the context of blanket design and materials properties. It is concluded that this inherently simple design could find application in both prototype and early commercial fusion reactors.

U.K.A.E.A. Research Group
Culham Laboratory
Abingdon
Berks.

August 1972.

C O N T E N T S

	<u>Page</u>
INTRODUCTION	1
FUSION REACTOR MODEL	1
FUSION REACTOR STRUCTURE	1
MAGNET SHIELD STRUCTURE	1
BLANKET STRUCTURE AND TRITIUM BREEDING GAIN	2
LITHIUM COOLING OF A FUSION REACTOR BLANKET	2
CELL STRUCTURE TEMPERATURES	3
STRESSES IN THE BLANKET STRUCTURE	3
CHOICE OF BLANKET STRUCTURE MATERIAL	3
CONCLUSION	4
ACKNOWLEDGEMENTS	4
REFERENCES	4

INTRODUCTION

First generation fusion reactors will use as fuel a mixture of deuterium and tritium, because it has by far the highest reaction rate at low plasma temperatures (1)*. Tritium is only present in nature in very small quantities, however, so that the amounts required must be produced artificially to maintain the fuel supply. This can be achieved by surrounding the plasma with a nuclear blanket comprised mainly of natural lithium, using (n,α) reactions in both ${}^6\text{Li}$ and ${}^7\text{Li}$ to breed tritium. With its low atomic mass lithium also has the advantage of being a good moderator, absorbing the energy of the 14 MeV neutrons from the D-T fusion reaction. Furthermore, lithium metal has excellent potential for heat transfer, being liquid between 186°C and 1380°C and having high specific heat and thermal conductivity. Conceptually, therefore, a lithium blanket surrounding the plasma would fulfill three essential functions - neutron moderation, tritium breeding and heat transfer. The application of this concept is discussed in the following sections.

FUSION REACTOR MODEL

The plasma in a fusion reactor must be isolated at all times from the materials of the surrounding blanket. Apart from the possibility of inertial

confinement (2), all proposals for plasma confinement use high magnetic fields, with field strengths up to 15 tesla. Various field configurations are possible, and this study considers a system based on Tokamak confinement, as illustrated in Fig.1 which shows a fusion reactor scaled for an output of about 5000 MW(t). The simplest Tokamak confinement system is assumed in which the magnetic field transform, or rotation, necessary for plasma equilibrium and stability is provided by diffusion driven currents (3), thus producing a 'steady state' plasma confinement system. As yet provision for auxiliary external magnetic fields, poloidal or vertical, and for any ignition, fuel injection and exhaust systems have been omitted.

As shown, the toroidal plasma volume is about 4 m minor diameter and 25 m major diameter. The toroidal magnetic field is provided by 32 separate superconducting magnet coils - each some 8 m diameter by 1 square metre cross section. A subdivided winding of this form seems most likely for practical reasons of manufacture and transport and to permit the necessary access between the coils to the nuclear blanket and plasma region. In addition to breeding and other functions already discussed, the nuclear blanket must also include structure and shielding material to limit the radiation damage to the stabilising conductors of the magnet winding.

*Numbers in parentheses designate References at end of paper

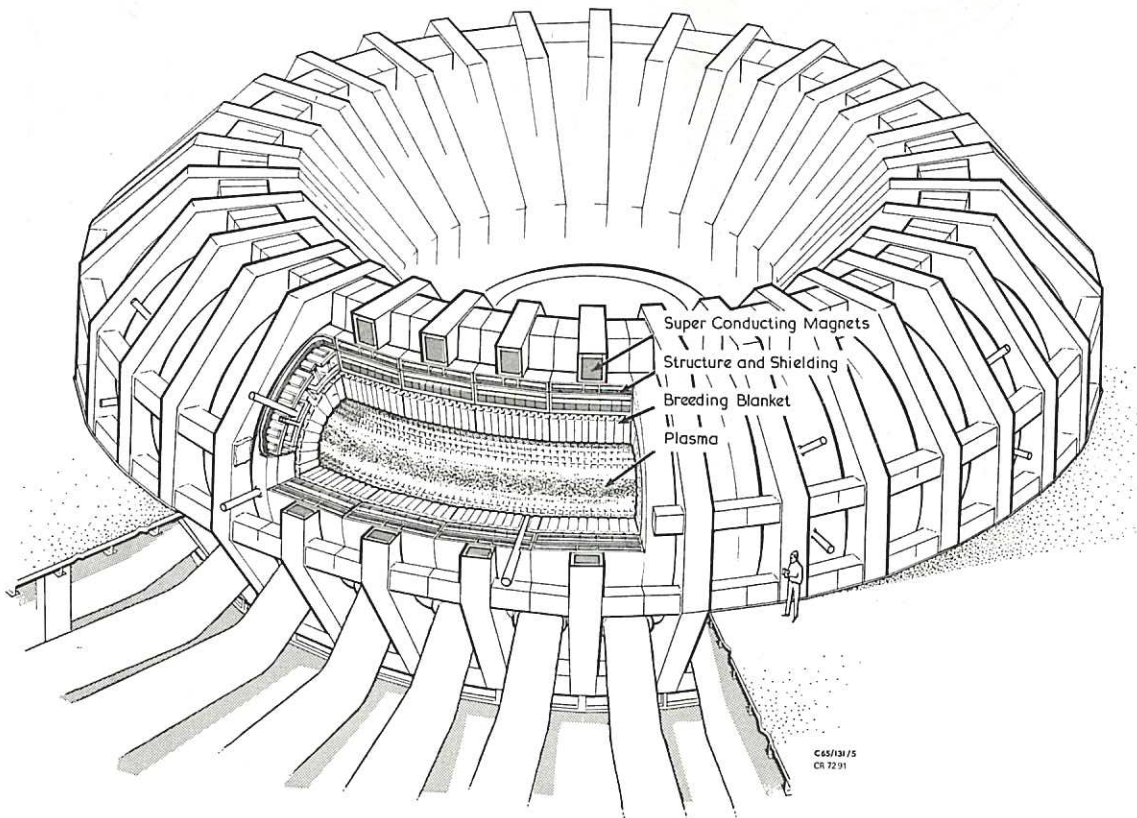


Fig.1 General view of a toroidal fusion reactor.

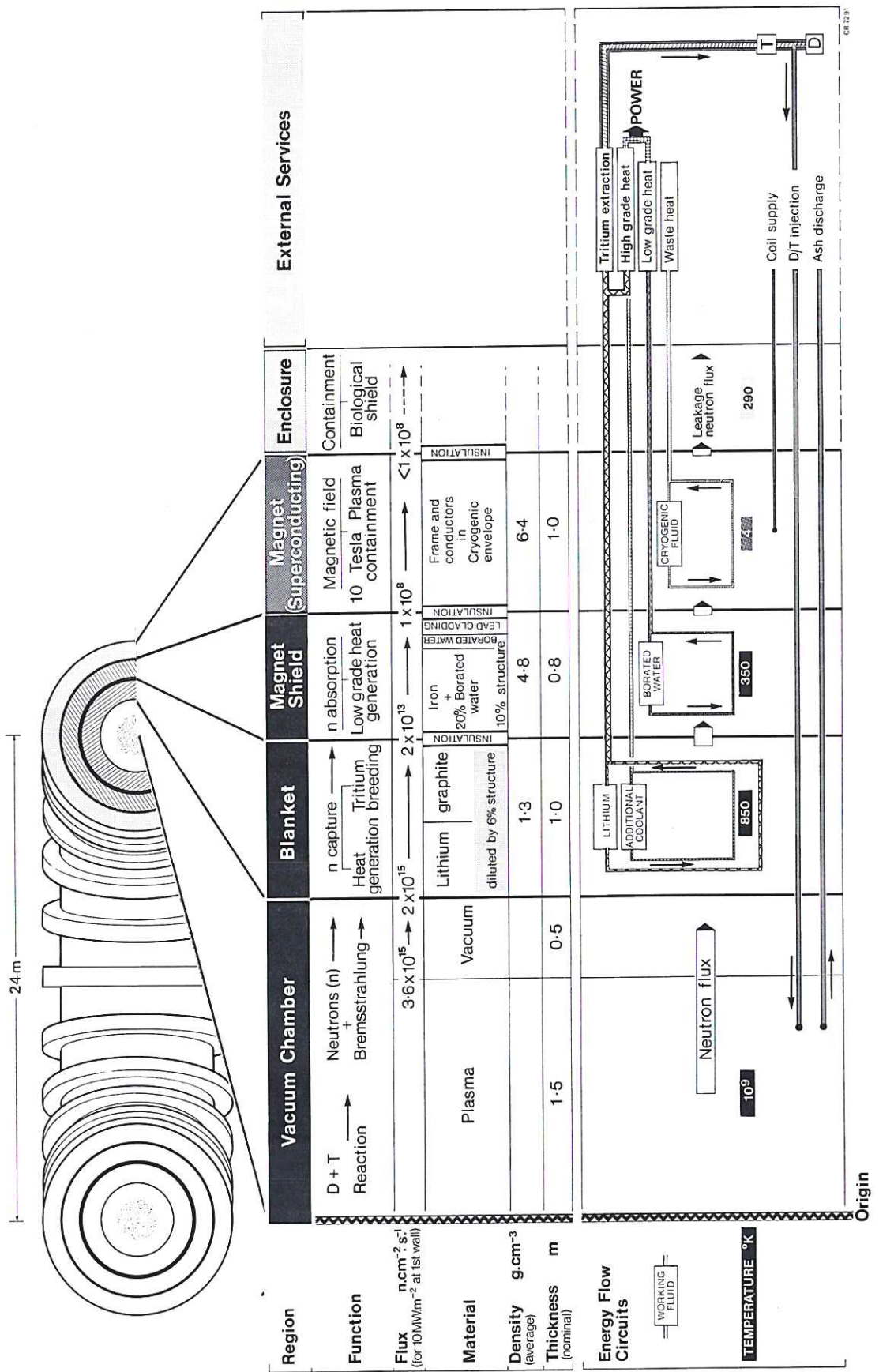


Fig.2 Fusion reactor blanket - structural design requirements.

The figure also indicates the principal limitations of the simple concept of a circulating lithium cooled fusion reactor blanket. Firstly the structural material required to contain the molten lithium near the plasma is limited to some 5 to 10% by volume in order not to reduce the tritium breeding gain. Secondly the lithium metal is itself a good electrical conductor and will experience high eddy current braking or magnetohydrodynamic (MHD) losses when it is circulated through the blanket. The purpose of this study has been to evaluate these limitations on the basis of this simple conceptual model of a fusion reactor structure.

power extraction. Points of particular importance for the engineering design of the different regions are:

1. In the nuclear blanket - the high neutron flux and resultant radiation damage rate, the low structure fraction and the high lithium temperature required for a reasonable thermal efficiency in the output turbo-alternator.
2. In the magnet shield - the high neutron flux attenuation to protect the magnet winding, the presence of iron ($\approx 50\%$ by volume), and the moderate service temperature.
3. In the superconducting magnet - the very low temperature (4 K) and need for cryogenic insulation, and the services access required through the magnet region. It would seem advisable to minimise physical contact between the cryogenic envelope of the magnet and any of the shield and blanket structure, piping etc.

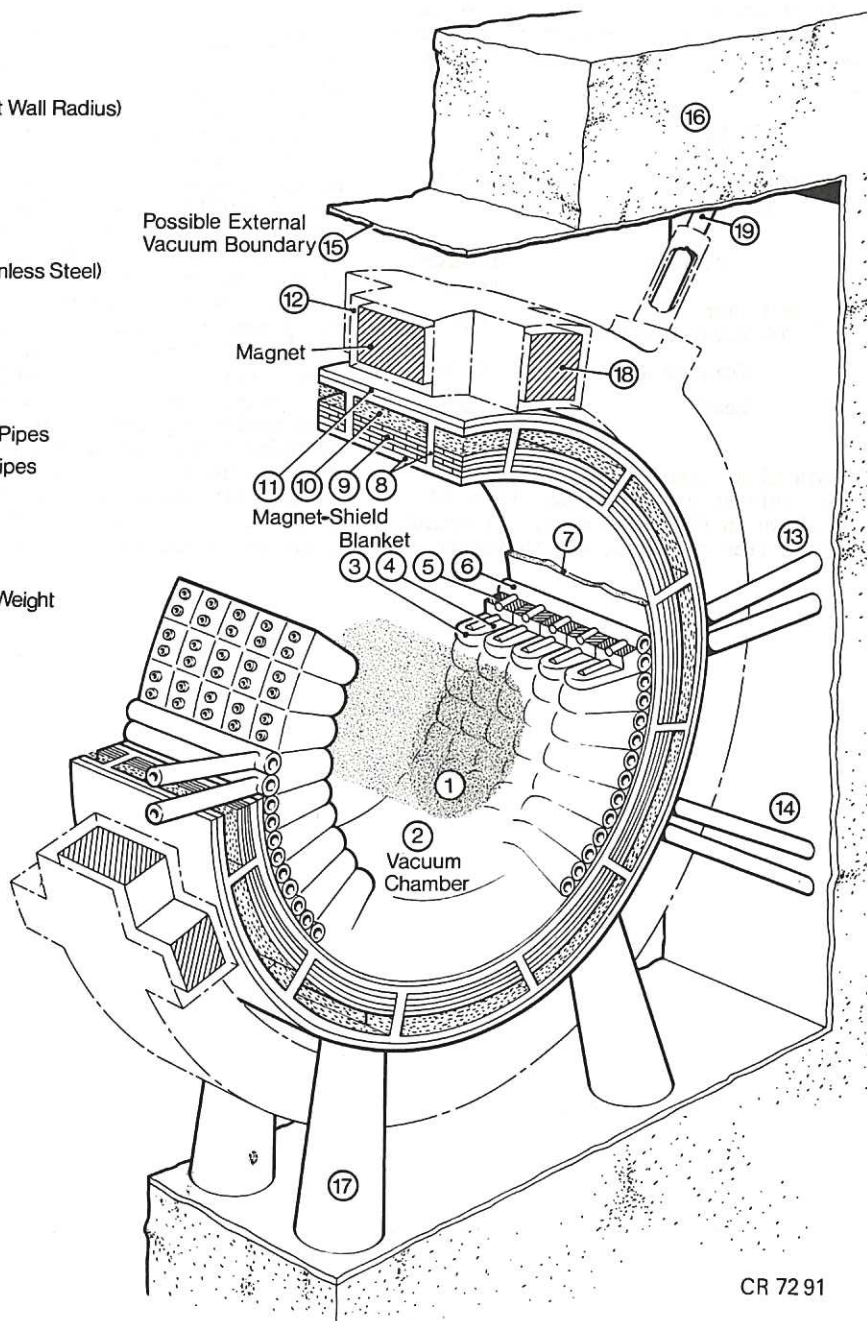
FUSION REACTOR STRUCTURE

The basic information and requirements for the structure design (4) are summarised in Fig.2 for the three principal regions - the blanket, the magnet shield and the magnet itself. The information is from nucleonic calculations (5) on tritium breeding, blanket heating, and shielding, materials properties and the necessary heat transfer and cooling circuits for

- 1 Plasma (15m Radius)
- 2 High Vacuum
- 3 Cell Structure (20m First Wall Radius)
- 4 Lithium
- 5 Graphite
- 6 Lithium Header
- 7 Thermal Insulation
- 8 Support Structure (Stainless Steel)
- 9 Iron
- 10 Borated Water
- 11 Lead Cladding
- 12 Cryogenic Envelope
- 13 Typical Blanket Coolant Pipes
- 14 Typical Shield Coolant Pipes
- 15 Containment Lining
- 16 Biological Containment

Restraints for:-

- 17 Magnet-Shield & Blanket Weight (Compressive)
- 18 Magnet Reaction Forces (Compressive)
- 19 Magnet Weight (Tensile)



CR 72 91

Fig.3 Fusion reactor blanket and magnet - general arrangement.

These features have been incorporated into the general arrangement of the structural design illustrated in Fig.3. This shows, in cylindrical geometry for simplicity, a short length of the reactor complete with its associated magnet coil supported within an outer biological shield. This latter could be the principal building structure if desired and as indicated might be an outer low vacuum boundary. The weight of the magnet coils would be supported quite independently of the rest of the structure by low thermal conductivity supports (Fig.3, item 19). It is assumed that the magnet reaction forces would be restrained by compressive members (item 18) within the cryogenic system (item 12) to minimise the refrigeration load.

MAGNET SHIELD STRUCTURE

The inner assembly (items 3 to 11) comprises the lithium blanket and magnet shield. This assembly would be located by compressive members (item 17) from the biological shield or building structure. Tensile members (not shown) could be included if necessary and these would all be located in the space between magnet coils. Shielding calculations have indicated that the required neutron flux attenuation ($\approx 5 \times 10^5$) would be obtained using the shield composition given in Table 1.

TABLE 1

Magnet Shield Composition for 5×10^5 Neutron flux Attenuation

LAYER	MATERIAL	THICKNESS metres
1	{ 80% Iron 20% Borated water	0.45
2	Borated water	0.05
3	Lead	0.05

A non-magnetic stainless steel structure can be incorporated into this shield, analogous to a submarine hull, as shown in Fig.3 (item 8). It would replace some of the iron and lead, and therefore

would have very little effect on the shielding efficiency of the assembly. Computer-aided design methods are available for such structures and it has been calculated that a simple structure of 20 mm thick stainless steel plate will support at conservative stresses, not only the vacuum forces but also all the mass loads of the shield and primary blanket—some 100 tonnes per metre length for the dimensions given in Fig.2. The volume of this 20 mm thick plate is about 20% of the iron shielding requirement. The remainder would be made up using blocks of a non-magnetic alloy (e.g. Fe + 13% Mn), but additional stainless steel could be substituted where local strengthening of the structure is required for load attachment points or penetrations. The borated water would be circulated through the shield to limit the temperature rise to $\approx 60^\circ\text{C}$ thus eliminating boiling and the possibility of pressurisation. Probably the most stringent requirement of the shield structure is to withstand the radiation damage of the neutron flux for its full working life. At a flux of 2×10^{13} neutrons/cm².s this is not a severe duty in comparison with structures in operating fission power reactors.

BLANKET STRUCTURE AND TRITIUM BREEDING GAIN

In Fig.3, the close nesting rectangular cells, the ducts containing the lithium, and the associated graphite reflector comprise the primary breeding blanket assembly. Fig.4 shows in more detail several views of a single cell using an alternative hexagonal cross section. Structurally the cell design would be a strong base carried by a beam from the magnet shield the base supporting the lightest possible body to minimise neutron absorption and loss of tritium breeding in the high neutron flux near the plasma. Depending on the location of the cell around the plasma the loading on the support beam varies from simple tension (or compression) to a normal cantilever. The beam would be designed to be as light as possible and of low thermal conductivity steel—thus minimising thermal loss to the shield. The graphite blocks would be similarly mounted from the magnet shield. For a cellular blanket of this form it has been shown (4) that the structure volume fraction, s , is equal to $2t_1/d_1$. In this way a correlation between tritium gain and pumping pressure

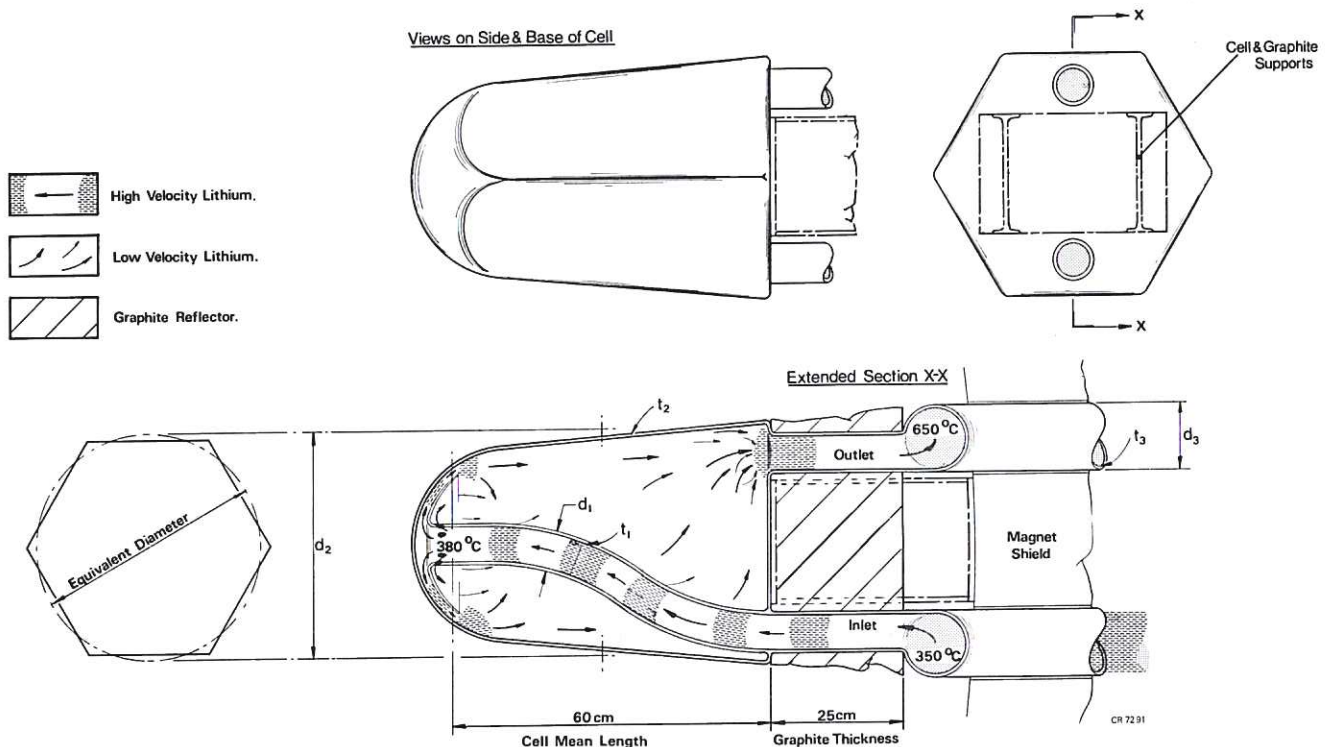


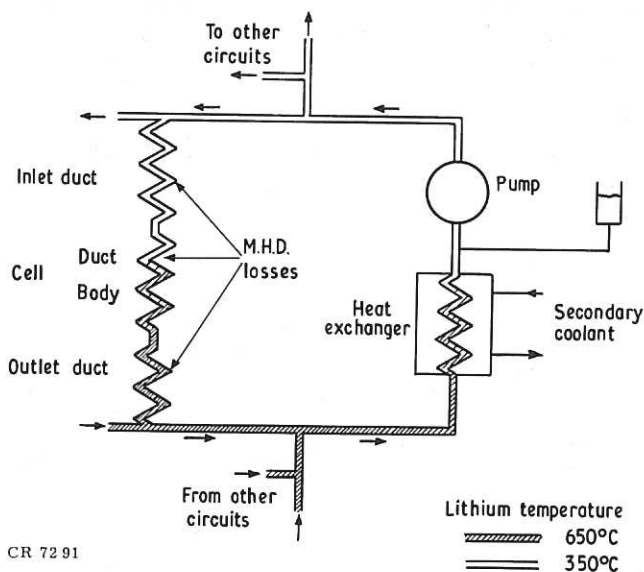
Fig.4 Hexagonal cell structure for lithium fusion reactor blanket.

can be developed from simple hoop stress considerations. The tritium breeding gain (= breeding ratio -1) has been calculated (5) for a cell 0.6 m long, 0.3 m diameter, at $s = 0.06$ of niobium with a graphite reflector of 0.2 m thickness. Allowing for the cooling ducts which pass through the graphite, but neglecting any other holes in the blanket, the gain of this relatively thin blanket is 0.3. No further optimisation has been done as this is considered ample to allow for the loss of breeding from fuel injection and exhaust holes of a final blanket design.

For convenience, the blanket cell model described has been based on circulating the lithium metal for cooling the blanket. Variations of blanket composition can be envisaged within the same structural concept and for example studies are in hand on a system using lithium beryllium fluoride eutectic ('flibe') as an alternative to the lithium metal. Separate cooling fluids can also be examined, e.g. helium, flowing in ducts in the cell walls and in the bulk lithium or 'flibe', yet still retaining the generalised cell model. Other features have also been considered: for example vacuum seals at the cell base, and for ducts penetrating the magnet shield. However, at this stage it is not necessary to develop designs beyond the point of demonstrating overall feasibility.

LITHIUM COOLING OF A FUSION REACTOR BLANKET

A simplified diagram of the cooling circuit is shown in Fig.5. The high pressure lithium from the pump is circulated through distribution ducting to the blanket cell and returns through similar ducting to the heat exchanger and pump. The heat exchanger forms the input to a secondary liquid metal circuit which delivers the heat energy to the steam boilers and turbines. The principal advantage of using a secondary circuit is the reduction of hydrodynamic losses in the primary circuit which is possible because of the high heat transfer coefficients and low pressure drops in liquid metal to liquid metal heat exchangers. The lithium flow paths between the magnet coils and through the shield are also indicated in Figs.3 and 4. It will be seen that the ducts are radially disposed between the coils, to minimise the duct length perpendicular to the field and give the best possible shielding of the coils from neutrons leaking from the blanket along the lithium in the ducts.



CR 72 91

Fig.5 Circuit schematic of lithium cooling system for a fusion reactor.

The MHD pumping losses and the pressure drop along the ducts containing the circulating lithium are caused by the fluid flow perpendicular to the magnetic field. Because of the reactivity of lithium with insulators

it is very probable that the duct walls in contact with the lithium will be metal. Thus, the electric currents induced by the lithium flow have a return path in the duct wall. Hunt and Hancox (6) have discussed MHD losses for flowing lithium in a fusion reactor blanket. Due to the pumping pressure required to overcome the MHD losses there is a limit to the product $P_{\omega} B_0^2$ where P_{ω} is the reactor thermal output per unit area of wall and B_0 is the average magnetic field in the plasma.

For a system with constant structure fraction, s , and one type of duct material, this limit is

$$P_{\omega} B_0^2 \leq 1.2 \times 10^5 (\Delta T \cdot \frac{1}{L} \cdot f/\sigma_{\omega}) \quad (1)$$

where $\Delta T(^{\circ}\text{C})$ = total bulk temperature rise of the lithium in the blanket

$L(\text{m})$ = the maximum effective path length of the lithium perpendicular to the magnetic field

$f(\text{N/m}^2)$ = highest stress in the duct material

$\sigma_{\omega}(\Omega\text{m})^{-1}$ = the electrical conductivity of the duct material.

The temperature rise, ΔT , in the lithium is determined by both the maximum allowable temperature in the blanket structure and the design of the heat engine. To keep the structure temperature below $\sim 700^{\circ}\text{C}$ and to suit steam conditions at the turbine stop valve of 2500 psi and 550°C , it is set at 300°C .

The effective path length, L , perpendicular to the magnetic field is given by the integral $\int (B/B_0)^2 dl$ along the actual lithium flow route, where B is the magnetic field perpendicular to the direction of flow. It therefore depends on the aspect ratio and dimensions of the magnetic field, the blanket thickness, and varies with position round the minor axis of the toroidal containment system. For the simplest case of radial flow of the lithium to the front of the blanket and back in the position of maximum local magnetic field in the inside or throat of the torus, $L \approx 10$ for a 2500 MW(e) reactor of the dimensions shown in Figs.1 and 2 and varies only slowly with change of the reactor output. A value of $L = 12$ has been used in the following calculations to allow for additional losses in paralleling manifolds, bends and fringe field effects.

The last term f/σ_{ω} is defined by the choice of duct material and is of obvious importance in determining the maximum usable wall loading P_{ω} at any particular magnetic field B_0 . Inserting the values for ΔT and L gives

$$P_{\omega} B_0^2 = 3 \times 10^6 f/\sigma_{\omega} \quad (2)$$

If design working stresses in the duct material are not to be exceeded, equation (2) sets maximum values for the product $P_{\omega} B_0^2$. Fig.6 shows curves of B_0 against P_{ω} for values of the 'stress/conductivity' ratio f/σ_{ω} of 50, 100 and 200. To achieve a useful life for the cell duct and wall material under high neutron irradiation and at temperatures of 700°C will most likely limit the maximum working stress to $\approx 100 \text{ MN/m}^2$ (15,000 psi). The wall conductivity will be approximately $10^6 (\Omega\text{m})^{-1}$ and therefore the maximum value of f/σ_{ω} is 100. The thick curve in Fig.6 shows this limit of magnetic field and wall loading in a lithium cooled fusion reactor.

There is a further limitation of P_{ω} and B_0 defined by plasma stability and equilibrium criteria (7), which in Tokamak geometry can be expressed in terms of the safety factor q - taken here as 2.5. The limit varies with the reactor output and Fig.6 includes curves for two ratings - a 250 MW(e) prototype assembly and a 2500 MW(e) commercial reactor. The intercepts between these and the MHD pumping

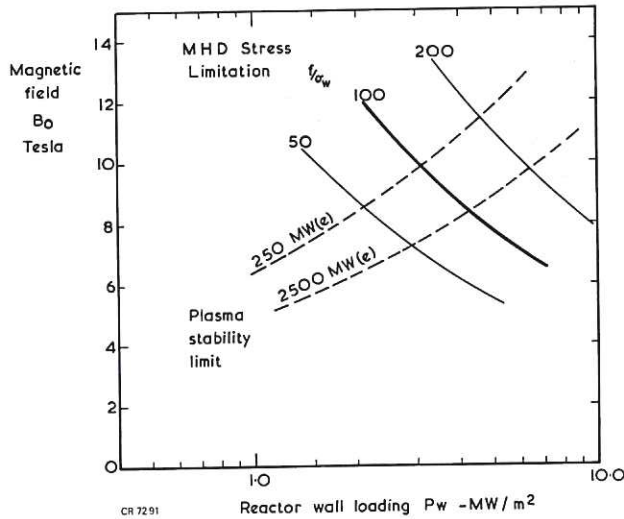


Fig.6 Curves of the limiting magnetic field as a function of the reactor wall loading defined by MHD loss consideration for a lithium cooled fusion reactor blanket. Also shown are the stability criteria for Tokamak plasma confinement.

loss curves define the maximum working wall loading for a particular reactor rating. The major reactor dimensions are also determined from simple geometrical relations between wall loading and output.

CELL STRUCTURE TEMPERATURES

Allowing for temperature differences between the structure and the lithium and across the heat exchangers, the maximum outlet temperature of the lithium is determined with reference to the high temperature creep properties of the structure. The temperature rise of the lithium in the blanket will then be determined from the associated heat engine design, and both of the lithium temperatures are independent of wall loading. In this study the lithium temperatures have been set at 350 °C at the inlet and 650 °C at the outlet. Local increases of the structure temperature above these lithium temperatures will occur for two reasons - direct nuclear heating of the structure and radiation loss from the plasma. Table 2 gives the results of calculations of the structure temperatures using nuclear heating data from reference 5 for the cell model of

TABLE 2

Lithium and Structure Temperatures in the Fusion Reactor Blanket Cell

POSITION	LITHIUM	NIOBIUM
	°C	°C
Entry to cell	350	-
At front of cell	373	419 (466)
At exit from front deflector	421 (445)	467 (538)
Rear exit from cell	650	≈ 717

Notes

1. Niobium temperatures are calculated for $P_w = 5 \text{ MW/m}^2$ and bremsstrahlung radiation of $0.02 P_w$
2. Cell dimensions: Overall diameter $d_1 = 0.3 \text{ m}$; Wall thickness $t_1 = 4.5 \text{ mm}$; Structure fraction $s = 0.06$
3. Figures in brackets are for wall thickness $t_1 = 9.0 \text{ mm}$

Fig.4. The lithium velocity was assumed to be maintained at the maximum duct velocity behind the front wall by means of suitable baffles inside the cell, but the lower return velocity through the body of the cell was used to calculate the rear wall temperature rise. These results are sufficiently encouraging to suggest that with detailed development very satisfactory structure cooling could be achieved by circulation of the blanket lithium in spite of the velocity limitations due to the MHD losses.

Without doubt, however, there remain problems of detail in the cell design. First, the pressure drop in the supply duct in the cell has been calculated neglecting the effect of the returning lithium outside the duct. It may be necessary to sandwich a layer of insulation between two metallic surfaces to form the duct wall, to provide the low duct conductance required, and, at the same time, protect the insulation from lithium corrosion. Secondly the magnetic field will prevent the cool fluid from the duct reaching the inner surface at the front of the cell, so that the coolant may be stagnant near the inside of the front wall, though this may not be serious because of the high thermal diffusivity of lithium. Finally, it may be necessary to eliminate sudden changes of section, e.g. at the exit from the cell, to ensure smooth streamline flow.

STRESSES IN THE BLANKET STRUCTURE

The significant stresses in the blanket cell structure are unquestionably due to the pressure required to maintain lithium circulation against the MHD losses. At a structure fraction of 0.06, and a cell diameter of 0.3 m, the cell wall thickness is 4.5 mm. The simple tensile stresses in this wall due to the mass load of 20 kg of lithium within the cell are negligible and there is always the possibility of introducing stiffening ribs with only a small change in structure fraction to resist any buckling. Then owing to the high heat capacity of the lithium, only low lithium flow velocities are required in the ducts, e.g. 15 cm/s at 10 MW/m² wall loading. In this case with ducts of only a few centimetres diameter and magnetic fields of 10 tesla, the MHD pressure drop exceeds the simple viscous drop by several orders of magnitude. As a result only two pressure/flow situations are of concern, the MHD controlled losses within the magnetic field and the normal turbulent flow losses in the external circuit. Estimating the external circuit losses from reference designs of sodium cooled fast breeder reactors gives the pumping power and pressure drop as ≈ 0.5% of electrical output and 250 kN/m².

In the fusion reactor magnetic field, the fractional pumping power to overcome the MHD losses in the lithium is given by

$$\frac{\text{Pumping power}}{\text{Reactor thermal output}} = \frac{\beta Q}{Q C_p \rho \Delta T} = \frac{f s}{1.21 \times 10^9}$$

where Q is the total lithium flow, and $C_p, \rho, \Delta T$ all refer to the lithium. For a maximum material stress, f , of 100 MN/m² and $s = 0.06$, the MHD losses are 0.5% of the reactor thermal output which is not excessive. Also $p = f s / 2 = 3 \text{ MN/m}^2$, and so the total pressure drop in the lithium flow system is ≈ 3.25 MN/m² (490 psi) - this is shown diagrammatically in Fig.7.

The maximum working stress which sets a limit to the product $P_w B^2$ in equation (2) occurs where the lithium flow first encounters the magnetic field. This is at the first inflection in curve A: with constant velocity flows in the ducts the MHD pressure gradient will be constant through the remainder of the system except for the low velocity return flow in the cell itself. The diagram shows clearly that for a constant structure fraction the working stress in the cell body will

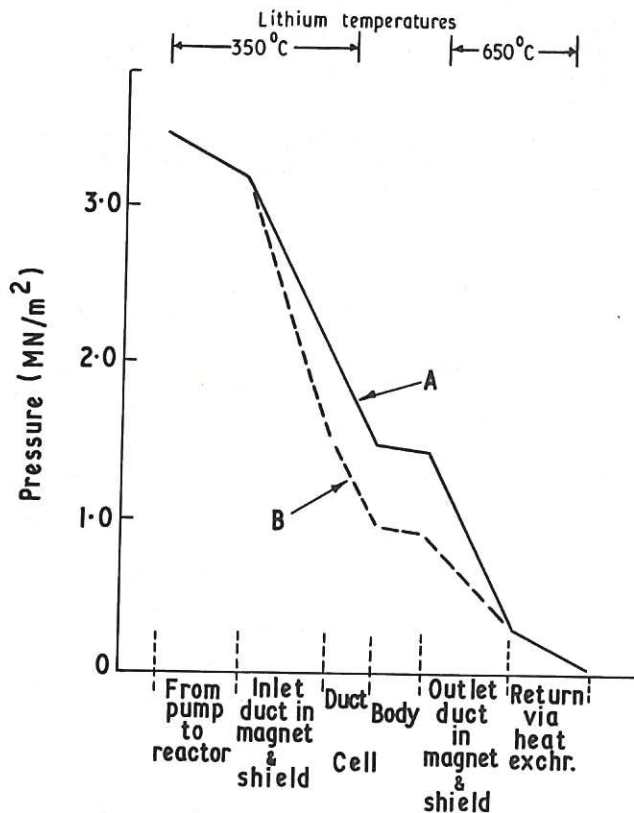


Fig.7 Diagram of primary circuit pressures in a lithium cooled fusion reactor. Curve A assumes σ_w constant whereas curve B shows the effect of temperature on the pressure drop and the reduced working pressure in the cell body.

be half that given by the total MHD loss calculation. However curve A is drawn for constant σ_w throughout the duct system. In fact because of the temperature difference between the inlet and outlet lithium, the pressure drop through the ducts cannot be constant, a higher drop occurs in the cooler inlet duct. The effect of this is shown in curve B and is to reduce the working stress and increase the design safety factor in the cell to ≈ 3 .

CHOICE OF BLANKET STRUCTURE MATERIAL

Molybdenum, niobium, and vanadium are all possible materials for fusion reactor blanket structures, because of their strength and corrosion resistance at high temperatures. For the lithium cooled system, however, where the control of MHD losses must be considered, it is also important that the material should have a high creep stress to conductivity ratio f/σ_w . Changes in this ratio during neutron irradiation under the working conditions in the blanket may also be important.

At the present time, creep stress data on vanadium and its alloys is not available, but would be of interest for fusion reactor studies because of the advantage of vanadium of low activity and afterheat (8). Molybdenum has a high creep strength, (9) but also has a high conductivity. The result is that at 750 °C the ratio $f/\sigma_w \approx 75$ which is lower than seems desirable from Fig.5. It would be interesting however if the ratio could be raised by alloying, to reduce the conductivity without affecting creep strength.

Niobium has for long been proposed for blanket structures particularly because of its corrosion resistance to lithium when alloyed with zirconium (10) and also for its relative ease of working. Many tritium breeding and blanket heating studies have also been done for lithium-niobium blankets (11). The 10^6 hr creep rupture strength and conductivity

for unirradiated Nb1%Zr and Nb5%Zr alloys are given in Table 3 at temperatures of 500 °C and 700 °C, i.e. for the front and rear of the cell body. This shows the importance of the ratio f/σ_w because Nb5%Zr is clearly the superior alloy due to both higher creep stress and lower conductivity.

TABLE 3

Creep Rupture Stress and Electrical Conductivity for Niobium Zirconium Alloys

ALLOY	TEST TEMPERATURE °C	10 ⁶ Hours RUPTURE STRESS (a) MN/m ²	CONDUCTIVITY (b) σ (Ωm) ⁻¹ x 10 ⁻⁶	f/σ_w
Nb1%Zr	500	> 230	2.7	> 85
	700	123	2.3	54
Nb5%Zr	500	270	1.3	210
	700	180	1.03	175

Note - (a) see reference 9;

(b) see references 12 and 13

From this data, if the lithium blanket system of a fusion reactor using Nb5%Zr structure is initially operated at a maximum $f/\sigma_w = 100$, it would have a safety factor at the front of the blanket cell of $3 \times \frac{210}{100} \approx 6$. At the rear of the cell the safety

factor would be reduced in the ratio 175/210, but the radiation damage rate in this region would be much lower than at the front of the cell (see Fig.2).

If these safety factors are sufficient to allow for the effects of neutron irradiation of the cell structure throughout an economically useful working life, the design wall loadings of lithium cooled fusion reactor blankets could be as indicated by the curve for $f/\sigma_w = 100$ (Fig.6). These wall loadings are an improvement on those suggested in our earlier studies (7) because the changes of parameters such as pressure and temperature throughout the lithium system have been considered.

The principal dimensions of a 250 MW(e) prototype fusion reactor and a 2500 MW(e) first generation commercial fusion reactor are given in Table 4 based on the intersection of the two criteria shown in

TABLE 4

Principal Reactor Dimensions

	UNITS	PROTOTYPE REACTOR	FIRST GENERATION COMMERCIAL POWER REACTOR
Reactor Electrical Output ($\eta = 0.43$)	MW(e)	250	2500
Thermal wall loading	MW/m ²	≈ 3.0 (2)	4.3
Major radius	metres	5.4	14.3
Wall radius	metres	1.13	3.0
Axial magnetic field (B_o)	tesla	9.75	8.4
Maximum magnetic field (\bar{B})	tesla	18.6	12.3
Coil aspect ratio		2.05	3.2
Average power density	kW(t)m ⁻³	180	680

Note 1: In both cases: Tokamak stability criterion $q = 2.5$; Plasma aspect ratio $R/a = 6$; Plasma/Wall radius ratio $r_p/r_w = 0.8$; Blanket plus shield thickness ≈ 1.5 metre

Note 2: The wall loading is lower than given by Fig.5 to correct for the assumption made for $\int (B/B_o)^2 d\ell$.

Fig.6. The maximum magnetic field in the prototype reactor is high due to the small magnet aspect ratio, and is probably higher than could be restrained by a reasonable mechanical support structure. For this reason lower magnetic fields and correspondingly lower reactor wall loadings would be used in the prototype so that the stresses due to the MHD pumping losses would no longer be a limitation. In the 2500 MW(e) commercial reactor the stresses become the major limitation, but by careful design it appears that acceptable wall loadings can be achieved.

CONCLUSION

An engineering design concept covering all the principal structural components for a fusion reactor blanket and magnet shield has been described. Much remains to be done to develop the design in detail, but at this stage of fusion reactor studies, it is only necessary to indicate overall feasibility. Other methods of cooling the blanket cells are now being studied but the overall simplicity of the direct lithium cooled fusion reactor blanket has much to commend it. In spite of the MHD losses the wall loading limitation is not severe and lithium cooling could have promising application for both prototype and early commercial fusion reactors.

ACKNOWLEDGEMENTS

The authors gratefully acknowledge the help which they have received in this study from their colleagues at the Culham Laboratory, and members of the Fusion Technology Study Group. Special thanks are due to Dr J C R Hunt (Cambridge University), M W George (A.E.R.E. Harwell), and J A Booth.

REFERENCES

1. D J Rose, On the feasibility of controlled fusion. ORNL-TM-2204, 1968.
2. L A Booth, Central station power generation by laser driven fusion. LA-4858-MS vol.1, 1972.
3. R J Bickerton, J W Connor and J B Taylor, Diffusion driven plasma currents and bootstrap tokamak. Nature Physical Science, vol.229, 110, 1971.
4. J T D Mitchell and M W George, A design concept for a fusion reactor blanket and magnet shield structure. To be published.
5. S Blow, Private communication, 1972.
6. J C R Hunt and R Hancox, The use of liquid lithium as a coolant in a toroidal fusion reactor. Part I, CLM-R 115, 1971.
7. R Hancox and J A Booth, The use of liquid lithium as a coolant in a toroidal fusion reactor. Part II, CLM-R 116, 1971.
8. D. Steiner, Long lived activities and radioactive waste management associated with D-T fusion reactors. Nuclear Fusion, vol.11, 307, 1971.
9. J B Conway and P N Flagella, Creep rupture data for the refractory metals to high temperatures. Gordon and Breach, New York, 1971.
10. J R DiStefano and A P Litman, Effects of impurities in some refractory metal-alkali metal systems. 20th Annual Conference of National Association of Corrosion Engineers, Chicago, 1964.
11. S Blow et al, Neutronics calculations for blanket assemblies of a fusion reactor. British Nuclear Energy Society Conference, 1969.
12. D V Rigney et al, The electrical resistivity of lithium and columbium-1 Zirconium alloy to 1430 °C, Pratt & Whitney Aircraft Co. Report, TIM-854, 1965.
13. Y Bychkov, et al, The normal elastic modulus of alloys of zirconium with niobium. Soviet Journal of Atomic Energy, vol.2, no.2, 1957.



